Proceedings of the ASME 2010 3rd Joint US-European Fluids Engineering Summer Meeting and 8th International Conference on Nanochannels, Microchannels, and Minichannels
FEDSM-ICNMM2010
August 1-5, 2010, Montreal, Canada

FEDSM-ICNMM2010-30828

Turbulent Two-Phase Flows and Particle Deposition in a Duct at High Concentrations

Goodarz Ahmadi*
Department of Mechanical and Aeronautical Engineering
Clarkson University
Potsdam, NY 13699

Hojjat Nasr
Department of Mechanical and Aeronautical Engineering
Clarkson University
Potsdam, NY 13699

John B. McLaughlin
Department of Chemical and Biomolecular Engineering
Clarkson University
Potsdam, NY 13699

ABSTRACT

Two-phase flows including particle-particle collisions and two-way coupling in a turbulent duct flow were simulated using a direct simulation approach. The direct numerical simulation (DNS) of the Navier-Stokes equation was performed via a pseudospectral method was extended to cover two-way coupling effects. The effect of particles on the flow was included in the analysis via a feedback force that acted on the fluid on the computational grid points. The point particle equation of motion included the Stokes drag, the Saffman lift, and the gravitational forces. Several simulations for different particle relaxation times and particle mass loading were performed, and the effects of the inter-particle collisions and two-way coupling on the particle deposition velocity, fluid and particle fluctuating velocities, particle normal mean velocity, and particle concentration were determined. It was found that when particle-particle collisions were included in the computation, the particle deposition velocity increased. When the particle collision was neglected but the particle-fluid two-way coupling was accounted for, the particle deposition velocity decreased slightly. When both inter-particle collisions and two-way coupling effects were taken into account in the simulations, the particle deposition velocity increased. Comparisons of the present simulation results with the available experimental data and earlier numerical results are also presented.

Keywords: DNS, Particle-particle collisions, particle deposition velocity, four-way coupling.

INTRODUCTION

Study of transport and deposition of aerosols in particle-laden flows is of considerable interest due to its importance in numerous industrial and environmental applications. Despite numerous experimental and computational studies, the interaction of particles with turbulence eddies is not fully understood.

Wang and Squires (1996) studied particle transport in fully developed turbulent channel flows using the one–way coupled LES simulation. They showed that the LES technique accurately predicted that the value of the streamwise fluctuating velocity of the particles was larger than that of the fluid. Zhang and Ahmadi (2000) used DNS to study aerosol particle transport and deposition in vertical and horizontal turbulent duct flows. They showed that the wall coherent structure plays an important role in the particle deposition process.

While most researchers ignored particle-particle interactions in their two-way coupling simulations, Yamamoto et al. (2001) studied the interaction between turbulence and solid particles in a fully developed channel flow using large eddy simulation; they also considered inter-particle collisions at high mass loadings. They showed that the shape and scale of particle concentrations calculated considering inter-particle collision are in good agreement with experimental observations of Fessler et al. (1994). Li et al. (2001) showed that particle-particle collisions greatly reduce the tendency of particles to accumulate near the wall. Recently, Nasr and Ahmadi (2007) studied the effect of two-way coupling and inter-particle collisions on turbulence modulation in a downward turbulent channel flow. They showed that when particle–particle collisions were included in the simulation, the predicted streamwise mean particle velocity profile became flatter than the fluid velocity profile due to transverse mixing, and as a result, turbulence attenuation occurred. Their simulation results were in good agreement with the experimental data of Kulick et al. (1994).

In this study, the effects of inter-particle collisions and two-way coupling on dispersed and carriers phase fluctuations were studied using the direct numerical simulation of the Navier-Stokes equation via a pseudospectral method. The particle deposition velocity, particle fluctuating velocities, particle normal velocity, and particle concentration profiles were evaluated under different conditions. The cases of one-way coupling, two-way coupling, four-way coupling, and inter-particle collisions without two-way coupling were analyzed. The effects of particle-particle collisions as well as two-way coupling on the simulation results are discussed.

GOVERNING EQUATIONS

The Lagrangian equation of motion of a spherical particle including the nonlinear drag and lift forces in wall units is given as

$$\frac{d\vec{u}^{+p}}{dt^{+}} = \frac{(1+0.15\,\mathrm{Re}^{0.687})}{\tau_p^{+}}(\vec{u}^{+f} - \vec{u}^{+p}) + \vec{L}^{+} \tag{1}$$

And

$$\frac{d\vec{x}^{+}}{dt^{+}} = \vec{u}^{+p} \tag{2}$$

where

$$\vec{x}^{+} = \frac{\vec{x}\,u^{*}}{\nu} \qquad t^{+} = \frac{t\,u^{*2}}{\nu} \qquad \vec{u}^{+} = \frac{\vec{u}}{u^{*}} \tag{3}$$

Here, u^{+p} is the non-dimensional particle velocity, u^{+f} is the non-dimensional instantaneous fluid velocity at the particle location, τ_p^{+} is the non-dimensional particle relaxation time, L^{+} is the non-dimensional lift force, and $\mathrm{Re}_p = d\left|u^f - u^p\right|/\nu$ is the particle Reynolds number based on the flow-particle slip velocity and the fluid kinematic viscosity, ν. (Note that only the y-component of lift force is considered in this study.) In equation (3), u^{*} is the flow shear velocity.

In equation (1), the non-dimensional particle relaxation time is defined as

$$\tau^{+} = S\frac{d^{+2}}{18} \tag{4}$$

here $d^{+} = du^{*}/\nu$ is the non-dimensional particle diameter and S is the particle-to-fluid density ratio. The non-dimensional component of the lift force in the y-direction is given as

$$L_y^{+} = 3.08\frac{du^{+}/dy^{+}}{Sd^{+}\left|du^{+}/dy\right|^{1/2}}(u^{+f} - u^{+p}) \tag{5}$$

It is assumed that when a particle is within one radius from the wall, it deposits with no rebound. To keep the particle concentration in the unchanged, when a particle is deposited on the wall, another particle is randomly introduced in the computational domain. The hard sphere particle-particle collision model with a coefficient of restitution equal to 0.95 was used in the analysis. The procedure for the numerical implementation of the particle-particle collisions as described by Li et al. (2001) was implemented in the present analysis. In this study, the collisions were assumed to be binary since multiple collisions are extremely rare at the particle concentrations that were considered.

The instantaneous fluid velocity field in the channel is evaluated by DNS of the Navier-Stokes equation using an additional source term due to the presence of particles. It is assumed that the flow is incompressible, and a constant mean pressure gradient in x-direction is imposed. The corresponding governing equations of motion are:

Continuity Equation: In this study the volume fraction of particles is very small, $\phi_v < 10^{-3}$; therefore, the continuity equation may be expressed as:

$$\nabla \cdot \vec{u}^{+f} = 0 \tag{6}$$

Momentum Equation: The effect of particles is added to the Navier-Stokes equations by an additional source term using the point force model:

$$\frac{D\vec{u}^{+f}}{Dt^{+}} = -\nabla^{+}p^{+} - \frac{dp^{+}}{dx^{+}}\hat{i} + \nabla^{+2}\vec{u}^{+} + S_{\vec{u}}^{p+} \tag{7}$$

where $\vec{u}^{f+} = (u^{f+}, v^{f+}, w^{f+})$ is the fluid velocity vector in wall units, and p^{+} is the pressure in wall units. The coupling between fluid and dispersed phases incorporated into the momentum equation via a feedback force per unit mass, which is the negative of the drag and lift forces acting on the particles exerted by the fluid in a certain computational cell; the particle feedback force per unit mass is given by

$$S_{\vec{u}}^{p+} = -\sum_{n=1}^{N^p}\frac{d\vec{u}^{p+}}{dt^{+}} = -\sum_{n=1}^{N^p}\left\{\frac{(1+0.15\,\mathrm{Re}^{0.687})}{\tau_p^{+}}(\vec{u}^{+f} - \vec{u}^{+p}) + \vec{L}^{+}\right\} \tag{8}$$

No-slip boundary conditions are assumed on the channel walls and periodic boundary conditions are imposed in the *x*- and *z*-directions as follows:

$$\vec{u}^{f+} = 0, \qquad y^+ = \pm H^+$$

$$\vec{u}^{f+}(x^+ + m\lambda_x{}^+, y^+, z^+ + n\lambda_z{}^+, t^+) = \vec{u}^{f+}(x^+, y^+, z^+, t^+) \quad (9)$$

where m and n are integers.

In this simulation a channel that has half-width H^+ in wall units, and a $\lambda_x{}^+ \times \lambda_z{}^+$ periodic segment in *x*- and *z*- directions is used. A schematic of the flow domain and the periodic cell are shown in Figure 1. A $nx \times ny \times nz$ computational grid in the *x*-, *y*- and *z*-directions is employed. The grid spacing in the *x*- and *z*- directions are constant, while the variation of grid points in the *y*-direction is determined by the collocation points of the Chebyshev series. The distance of the *i*th grid point in the *y*-direction from the centerline is given as:

$$y_i{}^+ = \frac{H^+}{2}\cos(\pi i / M), \quad 0 \le i \le M \qquad (10)$$

where $M = nz - 1$.

The channel flow code used in this study is the one developed by McLaughlin (1989). The code used a pseudo-spectral method for computing the fluid velocity field. That is, the fluid velocity is expanded in a three-dimensional Fourier-Chebyshev series. The fluid velocity field is expanded in Fourier series in the *x*- and *z*- direction, while in the *y*-direction a Chebyshev series is used. The code uses an Adams-Bashforth-Crank-Nickolson (ABCN) scheme to compute the nonlinear and viscous terms in the Navier-Stokes equation and performs three fractional time steps to advance the fluid velocity from time step (n) to time step (n+1). The details of the numerical techniques were described by McLaughlin (1989).

Typically, a temperature of 288 K, $\nu = 1.5 \times 10^{-5}\ N \cdot s / m^2$, and $\rho^f = 1.2\,kg/m^3$ for air were used. The friction velocity, u^*, was assumed to be 0.3 m/s. The channel half width was $H^+ = 125$ and the streamwise and spanwise periods were, respectively, $\lambda_x{}^+ = 630$ and $\lambda_z{}^+ = 630$. The numbers of grid points in the x-, y- and z-directions were *nx*=32, *ny* = 65 and *nz* = 64. The Reynolds number based on the friction velocity, u^*, and the half channel width was 125, while the flow Reynolds number based on the hydraulic diameter and the centerline velocity was about 8000. This condition corresponds to a channel half width, H = 12.5 mm, and streamwise and spanwise periods equal to 31.5 mm. The value for the density ratio, $S = \rho^p / \rho^f$, was taken to be 1000. Each simulation was performed for 2500 time steps, and the non-dimentional time step was chosen to be 0.2. Simulations were performed for particle diameters d = 25 and 30 μm ; the corresponding values of the non-dimensional particle relaxation time, are respectively, $\tau^+ = 14$ and 20.

Simulations were performed at particle mass loadings of M.L.=20% and 40%. It is important to note that for particles with $\tau^+ = 14$ and at M.L.=40%, approximately 600,000 particles were tracked. All results have been averaged over the simulation time, and over the streamwise and spanwise directions. Particles were uniformly distributed in the channel, and the initial velocity of each particle was set equal to the local fluid velocity evaluated at the center of the particle.

SIMULATION RESULTS:

In this section, simulation results for different particle parameters such as particle fluctuation velocities, particle streamwise and normal velocities, particle deposition velocity, and particle concentration are presented. To clarify the relative importance of various effects, all simulations were performed for four cases and the results are compared. These are: 1) One-way coupling; 2) two-way coupling; 3) four-way coupling (which is the physical case); and 4) including inter-particle collisions, but neglecting two-way coupling. Comparison of the results for different cases is used to assess the relative contributions of two-way coupling and inter-particle collisions on various particle velocity statistics.

Figure 2 shows a sample instantaneous velocity vector plot in the x-y plane at t^+=100 in the case of one-way coupling. The random deviations from the expected mean velocity are clearly seen from this figure. Figures 3-5 show the velocity field in the y-z plane at t^+ = 500 in the case of one-way and four-way coupling at mass loadings of M.L.=20% and M.L.=40%. The near wall coherent eddies and flow streams toward and away from the wall can be observed in these figures. Comparing the results for the one-way coupling in Figure 3 with the four-way coupling in Figures 4 and 5, it appears that the presence of solid particles damps the turbulence fluctuations and also decreases the number of eddies. These observations are in agreement with the experimental results of Rashidi et al. (1990). It is also seen that as particle mass loading increases, the level of damping increases.

The simulated root-mean square (RMS) fluctuation fluid velocities in the case of one-way and four-way coupling at mass loadings of 20% and 40% are shown in Figure 6. It is seen that, the addition of particles with $\tau^+ = 20$ attenuates the intensity of the fluctuations, and as particle mass loading increases, the level of attenuation increases. This trend is in agreement with earlier experimental data and numerical results. As was noted before, it has been widely shown that particles with diameter less than the Kolomogorov length scale attenuate the turbulence while particles with diameters larger than the Kolmogorov length scale augment it. In this study, the Kolmogorov scale varies from $\eta = 85$ μm at the wall to $\eta = 160$ μm at the channel centerline. The largest particle diameter tracked in the present study is 30 μm , which is smaller than the Kolmogorov length scale.

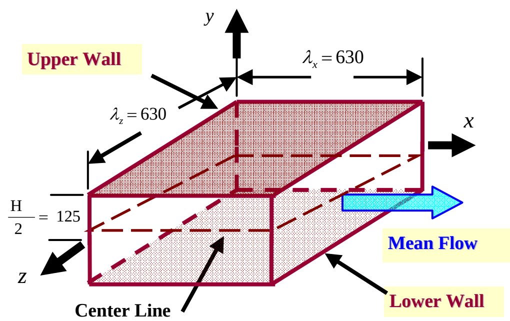

Figure 1 Schematics of the channel flow and computational periodic cell used.

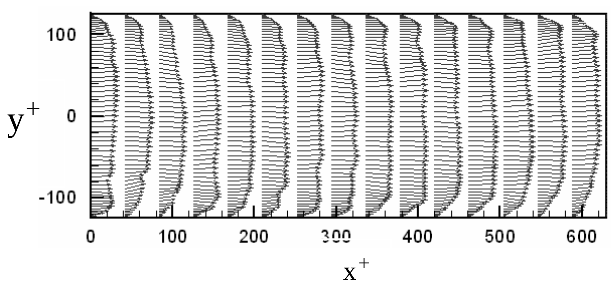

Figure 2 Sample velocity vector plot in x-y plane.

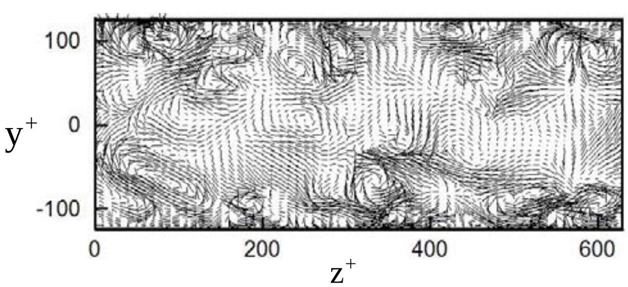

Figure 3 Velocity vector plot in y-z plane in presence of $\tau^+ = 20.0$ particles, one-way coupling.

Figure 7 shows the number of deposited particles versus time for particle relaxation time, τ^+, equal to 20 for different cases. Since in each case the number of particles is different, the number of deposited particles in this figure is normalized by the total number of particles being tracked.

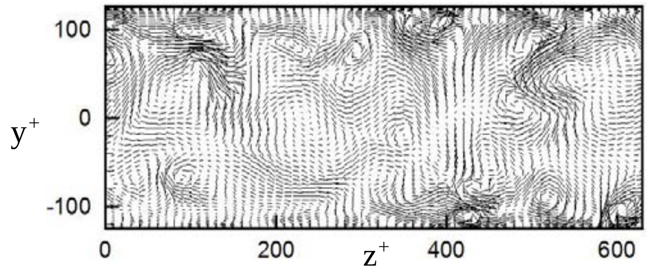

Figure 4 Velocity vector plot in y-z plane in presence of $\tau^+ = 20.0$ particles, four-way coupling at M.L.=20%.

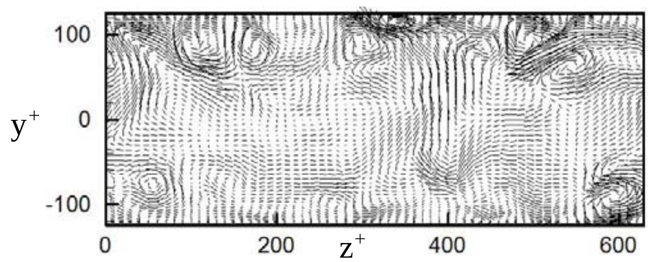

Figure 5 Velocity vector plot in y-z plane in presence of $\tau^+ = 20.0$ particles four-way coupling at M.L.=40%.

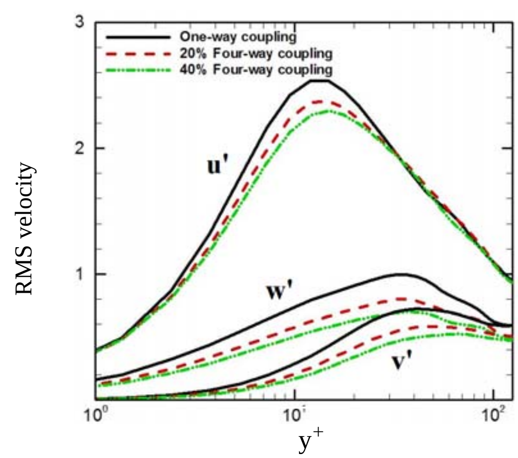

Figure 6 Effect of solid mass loading on the RMS velocities for M.L-=100% and 50 μm glass particles.

It is observed that in the case of two-way coupling (neglecting collisions), the number of deposited particles decreases and as particle mass loading increases. For the physical case, in which both the particle feedback force and inter-particle collisions are present, the number of deposited particles increases and as the particle mass loading increases. When the effect of particles on the flow is neglected but the inter-particle collisions are taken into account, the number of deposited particles increases even faster as particle mass loading increases. In summary for the range of parameters studied, the simulation results suggest that two-way coupling causes a decrease in the number of deposited particles, while inter-particle collisions lead to an increase in the number of deposited particles. The increase in the number of deposited particles due to inter-particle collisions is larger than the decrease caused by the two-way coupling effects. Thus, for the physical case (four-way coupling), the number of deposited particles increases with mass loading.

The simulations were also repeated for $\tau^+ = 20$, 35 and 50 and the results show similar trends. These simulation results are not shown here due to space limitations.

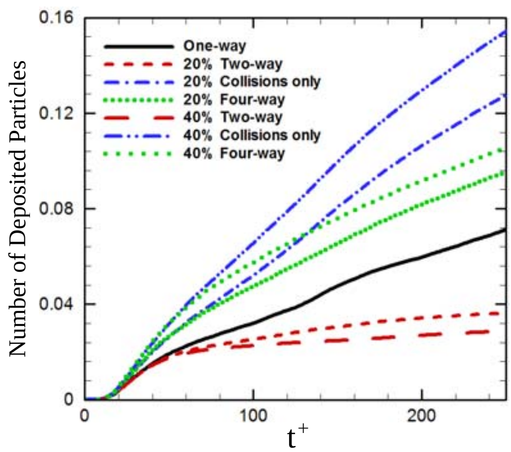

Figure 7 Normalized number of deposited particles versus non-dimensional time for particles with $\tau^+ = 20$.

Figure 8 shows the simulated non-dimensional deposition velocity, u_d^+, versus the non-dimensional particle relaxation time, τ^+ for different cases. The experimental data of Papavergos and Hedley (1982), the empirical equation of Wood (1981), and the simulation results of Li and Ahmadi (1992), McLaughlin (1989), He and Ahmadi (1999), and Zhang and Ahmadi (2000) and the empirical model prediction of Fan and Ahmadi (1993) for dilute suspensions are shown in this figure for comparison. The present simulation results for the one-way coupling case are in favorable agreement with the experimental data and earlier simulation results. It is observed that as the particle relaxation time increases, the particle deposition velocity increases.

Figure 8 also shows that the deposition velocity varies with the mass loading. In the physical case that both damping effects of particles and particle collisional effects are included (four-way coupling), the particle deposition velocity increases as the mass loading increases. When the particle collision effects are neglected in the simulations, the two-way coupling effects cause a decrease in the particle deposition velocity as turbulence is damped by the increase of particle mass loading. This figure also shows that the inter-particle collisions increase u_d^+ as mass loading increases. It is noteworthy to mention that particles with equal relaxation times, τ^+, may have different diameters and density ratios; this implies that particles with equal relaxation times behave differently when inter-particle collisions are included in the simulations.

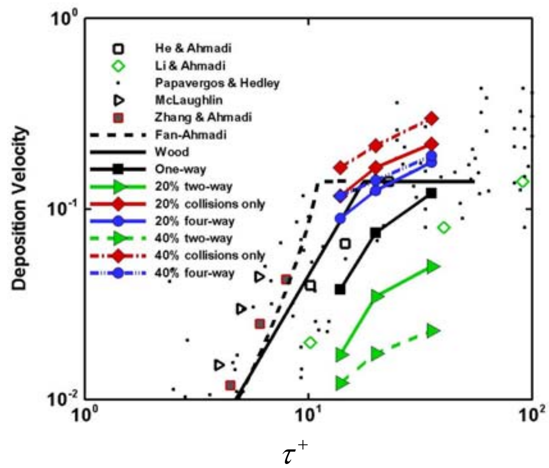

Figure 8 Non-dimensional particle deposition velocity versus non-dimensional particle relaxation time.

For particle deposition, the normal component of particle fluctuating velocity plays a crucial role. Figure 9 shows the root-mean square (RMS) normal fluctuating velocity of the airflow and particles with $\tau^+ = 14.0$ for different cases. Several features in this figure are noteworthy. The normal fluctuating velocity of particles in the case of one-way coupling is less than the fluid in the $y^+ > 10.0$ region and is greater than the fluid in the wall region ($y^+ < 10.0$). The decrease of the fluctuating velocity of the particles in the outer region is due to the fact that the inertial particles are not fully responsive to all turbulent eddies, and they fluctuate less than the flow. The increase of the normal fluctuating velocity of the particles in the wall region is perhaps due to the fact that, as a particle migrates toward the wall, it tends to retain the velocity that it possessed when being further from the wall. Therefore, a wide range of particle velocities is found in the wall region, causing an increase in the normal particle fluctuating velocity. Figure 9 shows that, for the case of two-way coupling (in the absence of collision), the particle normal fluctuating velocity is lower in the entire channel in comparison to the one-way coupling case, and also decreases as particle mass loading increases. This trend can be explained in terms of turbulence attenuation effects due to the presence of the particle feedback force as discussed before. When the particle feedback force is ignored but inter-particle collisions are included in the simulation, the particle normal fluctuating velocity increases in the entire channel compared with one-way coupling simulation, and as particle mass loading increases, the level of augmentation in particle normal fluctuating velocity increases. In the case of four-way coupling, the particle normal fluctuating velocity decreases in the outer region with $y^+ > 10.0$ and increases in the wall region with $y^+ < 10.0$ compared with the one-way coupling case. These results indicate that the two-way coupling effects decrease the particle normal fluctuating velocity, while inter-particle collisions enhance it.

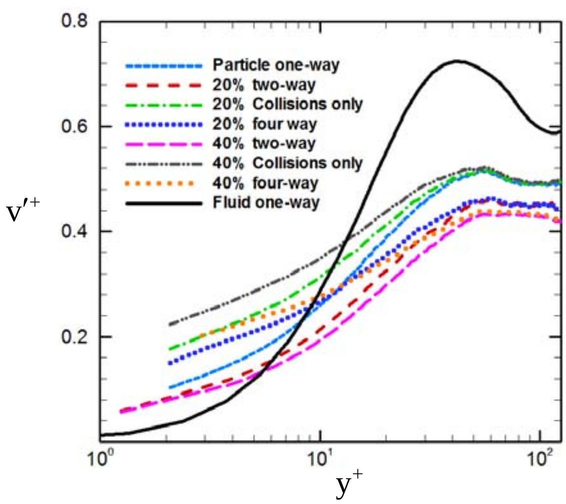

Figure 9 Normal fluctuating velocity versus the distance form the wall for particles with $\tau^+ = 20.0$

CONCLUSIONS

The effects of particle-particle collisions, two-way coupling and four-way coupling on particle deposition velocity, fluid and particle fluctuating velocity statistics, and particle concentration profile in a turbulent channel flow were studied. The time history of the instantaneous turbulent velocity vector was generated by the two-way coupled direct numerical simulation (DNS) of the Navier- Stokes equation via a pseudo spectral method. The particle equation of motion included the Stokes drag, the Saffman lift, and the gravitational forces. The effect of particles on the flow is included in the analysis via a feedback force on the grid points. The key findings of the study may be summarized as follows:

1) For the size ranges considered, the addition of particles attenuates the intensity of fluid turbulence fluctuations and as particle mass loading increases, the level of attenuation increases.

2) Inter-particle collisions increase the particle deposition velocity as mass loading increases, while two way coupling decreases it. In the physical case (four way coupling), the particle deposition velocity increases comparing with the one way coupling case.

3) Four-way coupling decreases the particle normal fluctuating velocity, v'^p, in the $y^+ > 10.0$ region and increases it in the wall region with $y^+ < 10.0$ compared with the one-way coupling case. The two-way coupling effects decrease the particle normal fluctuating velocity, while inter-particle collisions enhance it.

ACKKNOWLEDEMENT

The financial support of the Environmental Protection Agency (EPA) and the NYSTAR Center of Excellence is gratefully acknowledged.

REFERENCES

Chen, M., Y., McLaughlin, J. B., 1995, A New Correlation for the Aerosol Deposition Rate in Vertical. J. Colloid Interface Sci., 169, 437.

Fan, F. G., and Ahmadi, G., 1993, A sublayer model for turbulent deposition of particles in vertical ducts with smooth and rough surfaces. J. Aerosol Sci. 24, 45.

Fessler, J. R., Kulick, J. D. and Eaton J. K., 1994, Preferential Concentration of Heavy Particles in a Turbulent Channel Flow. Phys. Fluids., 6 (11): 3742-3749.

He, C. and Ahmadi, G., 1999, Particle deposition in a nearly developed turbulent duct flow with electrophoresis. J. Aerosol Sci. 30, 739.

Kulick, J. D., Fessler, J. R. and Eaton, J. K., 194, Particle response and turbulence modification in fully developed channel flow. Fluid Mech. 277, 109-134.

Li, A. and Ahmadi, G., 1992, Computer simulation of deposition of aerosols in a turbulent channel flow with rough wall. Aerosol Sci. Techno. 16, 209.

Li, Y., McLaughlin, J. B., Kontomaris, K., and Portela, L., 2001, Numerical Simulation of Particle-Laden Turbulent Channel Flow. Phys. Fluids., 13 (10): 2957-2967.

McLaughlin, J. B., 1989, Aerosol Particle Deposition in Numerically Simulated Turbulent Channel Flow. Phys. Fluids, A1, 1211-1224.

Nasr, H., and Ahmadi, G., 2007, The effect of two-way coupling and inter-particle collisions on turbulence modulation in a vertical channel flow. Int. J. Heat and Fluid Flow, 28(6), 1507-1517.

Papavergos, P. G. and Hedley, A. B., 1984, Particle deposition behavior from turbulent Flows. Chem. Eng. Des. 62, 275.

Rashidi, M., Hetsroni, G., and Banerjee, S., 1990, Particle-turbulence interaction in a boundary layer. Intl J. Multiphase Flow 16, 935-949.

Rousan, D. W. I. and Eaton, J. K., 2001, On the Preferential Concentration of Solid Particles in Turbulent Channel Flow, J. Fluid Mech., 428, 149-169.

Wang, Q. and Squires, K.D., 1996, Large eddy simulation of particle-laden turbulent channel flow. Phys. of Fluids, 8(5), 1207-1223.

Wood, N. B., 1981, A simple method for calculation of turbulent deposition to smooth and rough surfaces. J. Aerosol Sci. 12, 275.

Yamamoto, Y., Potthoff, M., Tanaka, T., Kajishima, T., and Tsuji, Y., 2001, Large- Eddy Simulation of Turbulent Gas-Solid Flow in a Vertical Channel: Effect of Considering Inter-Particle Collisions. J. Fluid Mech., 442, 303-334.

Zhang, H. and Ahmadi, G., 2000, Aerosol particle transport and deposition in vertical and horizontal turbulent duct flows. J. Fluid Mech., 406, 55-80.